Soft Magnetic Nanocrystalline Alloys for High Temperature Applications

Matthew A. Willard[1], Frank Johnson[2], John H. Claassen[1], Rhonda M. Stroud[1], Michael E. McHenry[2], and Vincent G. Harris[1]

1. U.S. Naval Research Laboratory, Materials Physics Branch, Code 6340, Washington, DC 20375, USA

2. Department of Materials Science and Engineering, Carnegie Mellon University, Pittsburgh, PA 15213, USA

Abstract

High temperature inductor applications require improved magnet performance, including simultaneous high magnetization and low core losses at ever higher operation frequencies. Conventional polycrystalline soft magnet alloys are mature technologies with little room for meaningful improvement. Recently, nanocrystalline soft magnetic materials possessing reduced hysteretic losses and offering higher operation frequencies than conventional alloys have been introduced. These nanocrystalline soft magnets with compositions Fe-Co-Zr-B-(Cu) have been offered as alternatives to the conventional alloys. This paper describes the processing, structure, and magnetic properties of these materials.

Keywords: high temperature magnets, nanocrystalline soft magnets, HITPERM

Report Documentation Page

Form Approved
OMB No. 0704-0188

1. REPORT DATE	2. REPORT TYPE	3. DATES COVERED
2002		**00-00-2002 to 00-00-2002**

4. TITLE AND SUBTITLE	5a. CONTRACT NUMBER
Soft Magnetic Nanocrystalline Alloys for High Temperature Applications	5b. GRANT NUMBER
	5c. PROGRAM ELEMENT NUMBER
6. AUTHOR(S)	5d. PROJECT NUMBER
	5e. TASK NUMBER
	5f. WORK UNIT NUMBER
7. PERFORMING ORGANIZATION NAME(S) AND ADDRESS(ES) **U.S. Naval Research Laboratory,Materials Physics Branch,Code 6340,Washington,dc,20375**	8. PERFORMING ORGANIZATION REPORT NUMBER
9. SPONSORING/MONITORING AGENCY NAME(S) AND ADDRESS(ES)	10. SPONSOR/MONITOR'S ACRONYM(S)
	11. SPONSOR/MONITOR'S REPORT NUMBER(S)

12. DISTRIBUTION/AVAILABILITY STATEMENT
Approved for public release; distribution unlimited

13. SUPPLEMENTARY NOTES
Mat. Trans. 43 (8): 2000-2005, (2002)

14. ABSTRACT
SEE REPORT

15. SUBJECT TERMS

16. SECURITY CLASSIFICATION OF:			17. LIMITATION OF ABSTRACT	18. NUMBER OF PAGES	19a. NAME OF RESPONSIBLE PERSON
a. REPORT **unclassified**	b. ABSTRACT **unclassified**	c. THIS PAGE **unclassified**	**Same as Report (SAR)**	**23**	

1. Introduction

High temperature inductor applications for power generation, conversion, and conditioning require improved soft magnetic materials. The desired materials characteristics for these applications include: low coercivity to minimize frequency independent losses, high resistivity to minimize frequency dependent eddy current losses, and high magnetization to increase the range of field amplitudes available for use. These properties are desirable for any inductor application, however, for high temperature applications the choice of materials is limited to those that possess sufficiently high Curie temperature and high magnetization at the operation temperature.

The aforementioned requirements for use at high temperatures restrict the composition of the alloys to those containing Fe and Co (e.g. Hiperco™ alloys). Carpenter Technology Inc.'s Hiperco™ alloys are FeCo-based steels, with alloying additions of V for ease of rolling the alloys and increasing the resistivity. The operation frequencies for these alloys are limited due to the thick sheets formed during processing (a few mm thick) and the low resistivity (~ 20 μΩ-cm for Hiperco27™), both of which increase eddy current losses. These conventional polycrystalline alloys present a mature technology with limited potential for more than incremental improvements.

One possible solution with potential for improvement of high temperature soft magnetic materials lies in the field of nanocrystalline alloys. These materials possess reduced hysteretic losses and improved high frequency range and response. This

paper focuses on the synthesis and properties of nanocrystalline soft magnets for high temperature applications.

2. Historical Background

In 1988, Yoshizawa, Oguma, and Yamauchi at Hitachi Metals, Ltd., developed the first nanocrystalline soft ferromagnetic alloy, called Finemet™.[1] The Finemet™ alloy, with compositions $Fe_{73.5}Si_{13.5}Nb_3B_9Cu_1$, consists of a two-phase microstructure in its optimally annealed condition. This microstructure is made up of a ferromagnetic $D0_3$-(Fe,Si) phase with grain diameters of 5 to 10 nm surrounded by a ferromagnetic amorphous matrix about 2 to 3 nm in extent. Shortly after the development of $Fe_{73.5}Si_{13.5}Nb_3B_9Cu_1$, Suzuki, et al. developed the Nanoperm™[2] alloy (e.g. $Fe_{88}Zr_7B_4Cu_1$), with a higher concentration of ferromagnetic transition metal than $Fe_{73.5}Si_{13.5}Nb_3B_9Cu_1$. The greater amount of Fe and the formation of α-Fe during primary crystallization provided increased magnetization of the $Fe_{88}Zr_7B_4Cu_1$ alloy. Both of these alloys are competitive with existing amorphous alloys, where high magnetization and ultrasoft magnetic properties are important. The $Fe_{73.5}Si_{13.5}Nb_3B_9Cu_1$ alloy shows lower loss characteristics than $Fe_{88}Zr_7B_4Cu_1$, but at the expense of magnetization.

Both of these alloys take advantage of characteristics from their two-phase microstructures. The amorphous phase provides a high resistance path to eddy current formation, thus increasing the possible operation frequency over the existing large-grained metallic alloys. Both of these characteristics warrant interest in these alloys, however they are not the most interesting characteristics.

The coercivity of the $Fe_{73.5}Si_{13.5}Nb_3B_9Cu_1$ alloy was found to contradict conventional alloy development paradigms. The reduction in grain size traditionally causes increased coercivity due to the pinning of domain walls by grain boundaries in the material. Nanocrystalline alloys, therefore, would have enormous coercivities by this reasoning. Astonishingly, the coercivities for these alloys were reduced as the grain size was reduced below the domain wall width.

3. Exchange Coupled Nanocomposites

Shortly after the discovery of the extraordinary soft magnetic properties of the $Fe_{73.5}Si_{13.5}Nb_3B_9Cu_1$ alloys, Herzer offered a theory for their behavior.[3] The idea was based on a random anisotropy model, used to explain anisotropy in amorphous magnetic alloys.[4),5)] The random anisotropy model considered atom pairs with non-periodic arrangements of bond directions, implying that the magnetocrystalline anisotropy of the amorphous alloy would differ from a crystalline alloy of the same composition due to the random orientations of the bonds. In its application to nanocrystalline alloys the small coercivity values are explicated by means of a volume average magnetocrystalline anisotropy.[3] The model requires the random orientation of nanocrystallites and grain sizes smaller than the exchange correlation length. An effective magnetocrystalline anisotropy replaces the bulk magnetocrystalline anisotropy, when these constraints are met. Using a coherent rotation model, the estimated coercivity is proportional to the grain size to the sixth power for grain sizes smaller than the exchange correlation length.

The model requires that the nanocrystallites remain exchange coupled to maintain the reduced coercivity. The exchange coupling of a ferromagnet becomes negligible when the Curie temperature is exceeded. In general, the Curie temperature of the amorphous phase is smaller than that of the crystalline phase thereby being the limiting factor for operation temperature. At operation temperatures exceeding the Curie temperature of the amorphous phase, the Herzer model is no longer valid and the coercivity of the nanocrystalline alloy increases. This presents a problem for all nanocrystalline alloys, but is amplified for Fe-based alloys where the amorphous phase Curie temperature is significantly depressed.

4. High temperature nanocrystalline soft magnets

As with conventional soft magnetic alloys for high temperature applications, the composition of nanocrystalline alloys is constrained to Co-based or (Fe,Co)-based alloys, owing to the Curie temperature of Co and its alloys. Although this restriction limits the choice of ferromagnetic compositions, there is still a great amount of flexibility in the design of new alloys for these applications. Flexibility in alloy design means alloys can be catered to specific applications, such as those requiring high permeability or low magnetostriction.

4.1 Alloy Design

Fabrication of nanocrystalline soft magnetic materials has been accomplished by standard rapid solidification techniques (i.e. melt spinning) followed by isothermal annealing above the primary crystallization temperature of the alloy. In general, the formation of nanocrystalline soft magnets by melt spinning is limited to compositions near deep eutectics where an amorphous precursor can be formed. Early transition metal (i.e. Zr, Hf, Nb), and metalloid elements (i.e. B, Si, P) have been employed to produce the deep eutectics in ferromagnetic transition metal systems. After melt spinning, optimal crystallization of the as-spun ribbons produces a two-phase microstructure with FCC, BCC and/or intermetallic nanocrystallites surrounded by a residual amorphous matrix. This two-phase microstructure is important because each phase improves the high frequency properties of the material. Specifically, the nanocrystallites provide high magnetization that allows for reduced sizes of the inductors and the residual amorphous phase provides high resistivity that dampens the eddy currents.

This technique has successfully allowed the formation of Fe-based, (Fe,Co)-based, and Co-based nanocrystalline alloys alike. However, the design issues of nanocrystalline alloys for high temperature applications are additionally constrained by the necessity of high Curie temperature of the residual amorphous phase. The (Fe, Co)-based nanocrystalline alloys maintain a high magnetization and Curie temperature allowing for higher operation temperatures than their Fe-based counterparts.

By varying the ratio of Fe/Co the magnetization and magnetocrystalline anisotropy can be controlled, however, reduction of the magnetostriction is difficult for the

highest magnetization alloys. The Co-based nanocrystalline alloys, on the other hand, possess high Curie temperature and low saturation magnetostrictive coefficients with reduced saturation magnetization.

Herzer's argument for the (Fe, Si)-based $Fe_{73.5}Si_{13.5}Nb_3B_9Cu_1$ alloys was a balance of the negative magnetostrictive coefficients for the crystalline phase by the positive coefficients for the amorphous phase to create a near zero magnetostrictive effect.[6] Another method of achieving near zero magnetostriction is to choose a composition where the nanocrystalline and amorphous phases have simultaneous near zero values. Indeed, a low magnetostrictive coefficient has been identified for both the amorphous and crystalline phases near 5 at% Fe in Co.[7]

Alloy ingots, with compositions $(Co_{0.5}Fe_{0.5})_{89-x}Zr_7B_4Cu_x$ (HITPERM) and $(Co_{0.95}Fe_{0.05})_{89-x}Zr_7B_4Cu_x$ (where x is 0 or 1), were prepared by arc melting high purity constituent elements (99.9+%). Ribbon samples were produced from the ingots by a single wheel melt-spinning process. The as-spun ribbons were approximately 2 mm in width, 20 to 40 μm in thickness, and several meters in length. Subsequent isothermal heat treatments above the primary crystallization temperature stabilized the nanocrystalline microstructure.

The $(Co_{0.5}Fe_{0.5})_{88}Zr_7B_4Cu_1$ alloy was designed to possess high Curie temperature and high magnetization.[8] The Fe/Co ratio of one to one was chosen to minimize the contribution of magnetocrystalline anisotropy to the hysteretic losses of the alloy. At this composition, the actual Curie temperature of the crystalline phase is never reached due to the polymorphic α-(BCC) to γ-(FCC) phase transformation at 985°C.

This first order phase transformation causes a precipitous drop in the magnetization, unlike that of the approach to the Curie temperature for most other ferromagnets (which are higher order transformations). This is a benefit for these alloys, as the magnetization does not appreciably decrease over a very wide temperature range. Another $(Co_{0.5}Fe_{0.5})_{88}Zr_7B_4Cu_1$ alloy composition of interest has an Fe/Co ratio of two to one, with the maximum saturation magnetization for the nanocrystalline phase and smaller magnetostrictive losses.[10] That being said, the magnetostrictive contributions to the losses of $(Co_{0.5}Fe_{0.5})_{88}Zr_7B_4Cu_1$ alloys are appreciable over the whole composition range due to the large values found in the nanocrystallites themselves.

The $(Co_{0.95}Fe_{0.05})_{89-x}Zr_7B_4Cu_x$ alloys were developed to provide a low saturation magnetostriction coefficient alloy with good high temperature properties.[11] In both bulk crystalline FCC-(Co, Fe) and in $(Co, Fe)_{80}B_{20}$ metallic glasses, the saturation magnetostrictive coefficients were found to change from positive values for Fe–rich compositions to negative values for Co–rich compositions near 5 at% Fe in Co.[8] At this zero crossing of the magnetostrictive coefficient, a nanocrystalline alloy could be formed with each phase maintaining a near zero magnetostrictive coefficient, provided that the composition of each phase did not greatly deviate from the overall composition of the alloy. Additionally, the relatively large magnetocrystalline anisotropy at this composition is reduced due to the nanocrystalline microstructure of the alloy.

4.2 Structural properties

Prior to annealing, as-spun ribbon samples were analyzed by differential thermal analysis (DTA) to determine crystallization temperatures. (Note: These and other techniques presented in this paper are described in detail elsewhere.)[8-11] The endothermic peaks correspond to the crystallization of phases from the amorphous phase. Figure 1 shows three peaks for the $(Co_{0.95}Fe_{0.05})_{89-x}Zr_7B_4Cu_x$ alloys, with about 150 °C between the primary crystallization (~ 500 °C) and the first secondary crystallization temperature. The primary crystallization for these alloys showed a combination of FCC and BCC grains by X-ray diffraction and transmission electron microscopy for a sample annealed at 550 °C. Wide spread nucleation occurs during the early stages of annealing. The nanocrystallites expel Zr and B as crystallization progresses, enriching and stabilizing the remaining amorphous phase. This reaction is what allows the fine-grained microstructure to develop. At sufficiently high temperatures, the remaining amorphous phase crystallizes into $(Co,Fe)_3Zr$ and other phases that are detrimental to the magnetic properties. At the same time, the removal of the stabilized amorphous phase allows the existing primary nanocrystallites to begin growing again, with further magnetic property degradation.

The phases formed during crystallization were determined by X-ray diffraction (XRD). Figure 2 shows the XRD patterns for the $(Co_{0.95}Fe_{0.05})_{89}Zr_7B_4$ alloy after isothermal annealing at 550, 650, and 750°C for one hour each. The sample annealed at 550°C for each alloy showed Bragg peaks from both BCC (identified by dots in Figure 2) and FCC crystallites. The BCC peaks vanished for samples annealed at higher temperatures, indicating that the formation of the FCC is more stable than the BCC, although they are both close in formation energy. The implication for the magnetic properties of the two primary crystallites is unclear at this time. At

annealing temperatures above secondary crystallization, the formation of $(Co,Fe)_3Zr$ and $(Co,Fe)_2Zr$ phases form, as indicated by the XRD pattern for the sample annealed at 750 °C. Examination of the peak width broadening due to the grain size of the crystallites reveals increased grain growth at higher annealing temperatures (as summarized in Table 1).

Transmission electron microscopy (TEM) was used to image the microstructure of these alloys and analyze the phases present. Figure 3 provides a high resolution TEM image of the nanocrstallites for the $(Co_{0.95}Fe_{0.05})_{88}Zr_7B_4Cu_1$ alloy annealed at 550 °C for 1 hour. This sample has an average grain size of about 7 nm with a 2 to 3 nm intergranular amorphous phase. The grains have nearly spherical shape and uniform size.

The crystallization behavior and microstructure of these alloys are similar to those of the Fe-based nanocrystalline alloys that have excellent soft magnetic properties. The differences between the Fe-based nanocrystalline alloys and the (Co,Fe)-based ones are found when the magnetic properties are examined.

4.3 Magnetic properties

Direct current magnetic hysteresis loops were collected using a vibrating sample magnetometer (VSM) at room temperature. The hysteresis loops for as-spun and annealed samples of $(Co_{0.95}Fe_{0.05})_{88}Zr_7B_4$ are presented in Figure 4. The loops reflect the microstructure of the samples, showing higher coercivities for alloys annealed at higher temperatures. The coercivity increases due to increased average grain size and

formation of secondary phases that act as to pin domain walls. The influence of secondary phases is most evident in the sample annealed at 750°C where a shoulder has developed in the second quadrant of the loop. This is indicative of the reduction in exchange coupling between the primary and secondary crystallites. As indicated in the high field regions, the alloy annealed at 550°C shows a slightly higher saturation magnetization due to the formation of the crystalline phase. This effect is more pronounced in Fe-based alloys where the difference between the magnetization of the amorphous and crystalline phases is greater. At the highest annealing temperature, the saturation magnetization is slightly lower than the optimally annealed sample. This is presumably due to the formation of the secondary phases at the expense of some of the primary crystalline phase.

Thermomagnetic data were collected using a VSM with a furnace attachment. An as-spun $(Co_{0.5}Fe_{0.5})_{88}Zr_7B_4Cu_1$ sample was examined by this method to a maximum temperature of 1000 °C. Where Fe-based nanocrystalline materials succeed at producing low coercivity at room temperature, they fail to maintain that behavior at high temperatures, due to the reduced Curie temperature of the amorphous phase between the nanocrystallites. As the operation temperature surpasses the amorphous phase Curie temperature, the nanocrystallites decouple from one another resulting in an increased coercivity. Therefore, for nanocrystalline alloys to function at high temperatures, the intergranular amorphous phase must possess a high Curie temperature.

The (Fe, Co)-based alloys have addressed this issue by producing an amorphous phase having a Curie temperature greater than the primary crystallization temperature.

First-principles calculations of the magnetic moment in equiatomic FeCo suggest a Curie temperature in excess of 1500 K[12]. (This value is inaccessible to experimentation due to the previously mentioned α to γ phase transformation.) Thermomagnetic measurements of the amorphous precursors to $(Co_{0.5}Fe_{0.5})_{88}Zr_7B_4Cu_1$ show the magnetization of the amorphous phase persists until the primary crystallization temperature.[9),11)] It is reasonable to assume that the orbital angular momentum of the transition metal atoms in the amorphous phase is effectively quenched and that only spin angular momentum (S) contributes to the moment, J. Hence, the thermomagnetic behavior of amorphous $(Co_{0.5}Fe_{0.5})_{88}Zr_7B_4Cu_1$ can be fit to a spin only Brillouin function (J=±S), yielding values for the internal field and magnetic moment. The function can be extrapolated to high temperatures to give an estimate of the Curie temperature. The $(Co_{0.5}Fe_{0.5})_{88}Zr_7B_4Cu_1$ amorphous alloys are estimated to have Curie temperatures in the range of 800 °C to 850 °C. The Curie temperature of the amorphous phase will change after crystallization due to segregation of the alloying elements. Figure 5 shows thermomagnetic data for a $(Co_{0.5}Fe_{0.5})_{88}Zr_7B_4Cu_1$ sample initially in the amorphous state. The amorphous material retains its magnetization beyond 475 °C, the temperature at which the nanocrystalline grains precipitate from the amorphous matrix. The $Fe_{88}Zr_7B_4Cu_1$ alloy, also shown in Figure 5, shows a low Curie temperature of the amorphous phase making high temperature use of this alloy impossible.

In operation, when the Curie temperature of the amorphous phase at the grain boundaries is surpassed, the nanocrystallites decouple. The coercivity increases as the nanocrystalline grains approach a superparamagnetic state at a temperature far

below the Curie temperature of the nanocrystallites. This behavior occurs in the Fe-based alloys for operation temperatures approaching 300 °C.

Magnetostriction measurements were made by monitoring strain with a commercial strain gage glued between a pair of ribbons while rotating the ribbon through a saturating field. The applied field during the magnetostriction measurement surpassed the shape anisotropy of the ribbons, in both the easy and hard directions. Figure 6 shows magnetostriction data collected in this manner. This technique avoids the need for a ideally demagnetized state as a reference point for measurement. By this method, the saturation magnetization, λ_s, is given by 2/3 $\Delta(\delta l/l)$.[13] This yields a value of 11.5 ppm for the $(Co_{0.95}Fe_{0.05})_{88}Zr_7B_4$ alloy annealed at 550 °C for 1 hour.

The development of Co-based alloys provides the high Curie temperature due to the Co-rich composition. As found by O'Handley[8], a composition region near 5 at% Fe in Co exhibits simultaneous low values of the magnetostrictive coefficients for the crystalline and amorphous phases. This influenced the composition of these alloys, with the expectation that the composition of the crystalline phase would not change appreciably from that of the overall composition.

The magnetostrictive coefficients are not as close to zero as anticipated. The saturation magnetostrictive coefficient for the $(Co_{0.95}Fe_{0.05})_{89-x}Zr_7B_4Cu_x$ alloys after annealing at 550 °C for one hour are 11.5 and 13.5 ppm, for x=0 and x=1 respectively. This is most likely due to local composition deviations from the overall composition of the alloy during crystallization. Presumably, modifications to the

composition of the starting material and annealing temperature or time variations might be used optimize the alloy.

6. Conclusions/Summary

(Fe,Co)-based nanocrystalline alloys with a uniform grain size of 10 to 15 nm have been produced by rapid solidification processing with subsequent optimal isothermal heat treatment. The primary crystalline phase has a BCC and/or FCC crystal structure. Operation temperatures are not inhibited by decoupling of the nanocrystallites due to the elevated Curie temperature of the residual amorphous phase. This allows the alloys to operate at temperatures as high as 600 °C. Co-based nanocrystalline alloys with saturation magnetostrictive coefficients of 11.5 ppm have been produced for high temperature operation.

Nanocrystalline materials exhibiting soft magnetic properties have great potential for high temperature applications. Continual improvements to the alloy composition and processing conditions will provide improved properties and stability of these alloys. In the future, developing zero magnetostrictive (Fe,Co)-based alloys may be possible with improved magnetization and lower losses.

Acknowledgments

MAW and VGH gratefully acknowledge the support of the Office of Naval Research. MEM and FJ gratefully acknowledge the support of ABB Corporation and the Air Force Office of Scientific Research, Air Force Materiel Command, USAF, under

Grant No. F49620-96-1-0454. FJ acknowledges NASA Graduate Student Researcher Fellowship program under Grant No. NGT3-52379. MAW acknowledges the National Research Council Research Associateship program.

References

1) Y. Yoshizawa, S. Oguma, and K. Yamauchi, J. Appl. Phys. **64** (1988) 6044-6046.
2) K. Suzuki, M. Kikuchi, A. Makino, A. Inoue, and T. Masumoto, Mat. Trans. JIM **32** (1991) 961-968.
3) G. Herzer, IEEE Trans. Mag. **26(5)** (1990) 1397-1402.
4) R. Harris, M. Plischke, and M. J. Zuckermann. Phys. Rev. Lett. **31(3)** (1973) 160-162.
5) R. Alben, J. J. Becker, and M. C. Chi. J. Appl. Phys. **49(3)** (1978) 1653-1658.
6) G. Herzer, Physica Scripta **T49** (1993) 307-314.
7) R. C. O'Handley, Solid State Comm. **21** (1977) 1119-1121.
8) M. A. Willard, D. E. Laughlin, M. E. McHenry, D. Thoma, K. Sickafus, J. O. Cross, and V. G. Harris, J. Appl. Phys. **84** (1998) 6773-6777.
9) F. Johnson, P. Hughes, R. Gallagher, D. E. Laughlin, M. E. McHenry, M. A. Willard, and V. G. Harris, IEEE Trans. Mag., **37** (2001) 2261-2263.
10) M. A. Willard, J. H. Claassen, R. M. Stroud, and V. G. Harris, J. Appl. Phys. (2002), in press.
11) M. A. Willard, *Structural and Magnetic Characterization of HITPERM Soft Magnetic Materials for High Temperature Applications*, Ph.D. Thesis: Carnegie Mellon University, 2000.
12) J. M. MacLaren, T. C. Schulthess, W. H. Butler, R. A. Sutton, and M. E. McHenry, J. Appl. Phys., **85** (1999) 4833-4835.

13) A. Datta, D. Nathasingh, R. J. Martis, P. J. Flanders, and C. D. Graham, Jr., J. Appl. Phys. **55(6)** (1984) 1784-1786.

Table 1: Structural and magnetic properties of $(Co_{0.95}Fe_{0.05})_{88}Zr_7B_4Cu_1$ and $(Co_{0.95}Fe_{0.05})_{89}Zr_7B_4$ nanocrystalline alloys. Annealing times were one hour for all annealed samples. Grain size (D) was determined by Scherrer analysis of Bragg peaks. Samples with asterisks indicate the presence of amorphous phase as determined by XRD and/or TEM.[11)]

Alloy	Anneal Condition	a_0 (Å)	Phase	D (nm)	m_s (emu/g)	H_c (Oe)
$(Co_{0.95}Fe_{0.05})_{88}Zr_7B_4Cu_1^*$	As-spun	-		N/A	139.3	0.06±0.1
$(Co_{0.95}Fe_{0.05})_{88}Zr_7B_4Cu_1^*$	550 °C	3.552	FCC	10±3	142.2	0.26±0.1
		2.834	BCC	10±1		
$(Co_{0.95}Fe_{0.05})_{88}Zr_7B_4Cu_1$	600 °C	3.555	FCC	16±2	127.4	33±0.1
$(Co_{0.95}Fe_{0.05})_{88}Zr_7B_4Cu_1$	650 °C	3.559	FCC	16±3	131.6	53±0.1
$(Co_{0.95}Fe_{0.05})_{88}Zr_7B_4Cu_1$	700 °C	3.554	FCC	16±2	127.0	90±0.1
$(Co_{0.95}Fe_{0.05})_{88}Zr_7B_4Cu_1$	750 °C	3.557	FCC	23±3	130.1	160±0.1
$(Co_{0.95}Fe_{0.05})_{89}Zr_7B_4^*$	As-spun	-		N/A	138.8	0.47±0.1
$(Co_{0.95}Fe_{0.05})_{89}Zr_7B_4^*$	550 °C	3.569	FCC	17±3	140.7	1.6±0.1
		2.835	BCC	9±1		
$(Co_{0.95}Fe_{0.05})_{89}Zr_7B_4$	650 °C	3.555	FCC	17±2	137.6	68±0.1
$(Co_{0.95}Fe_{0.05})_{89}Zr_7B_4$	750 °C	3.555	FCC	23±3	134.4	180±0.1

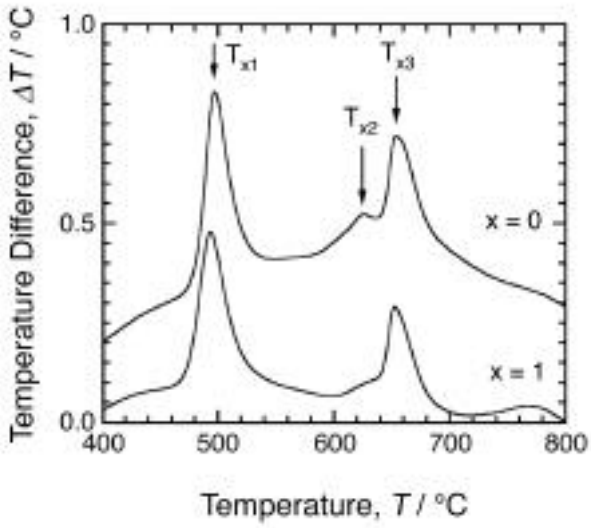

Figure 1: Differential thermal analysis of the as-spun $(Co_{0.95}Fe_{0.05})_{89-x}Zr_7B_4Cu_x$ alloys with a heating rate of 20 °C/min.

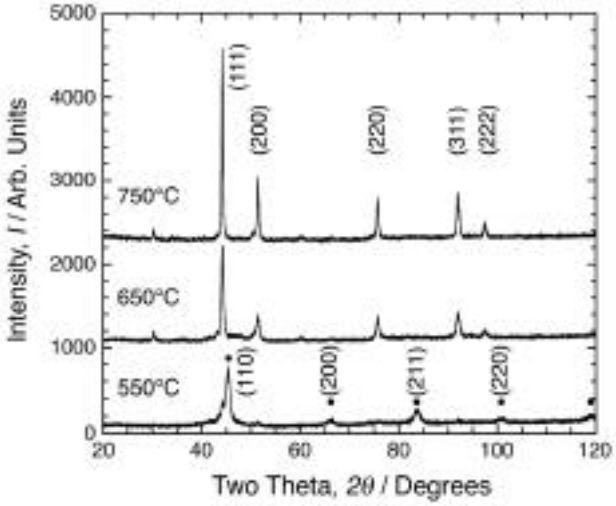

Figure 2 X-ray diffraction data for $(Co_{0.95}Fe_{0.05})_{89}Zr_7B_4$ samples annealed at 550, 650 and 750°C for one hour. Indexing of the diffraction patterns include dots for the BCC peaks and no dots for FCC peaks.

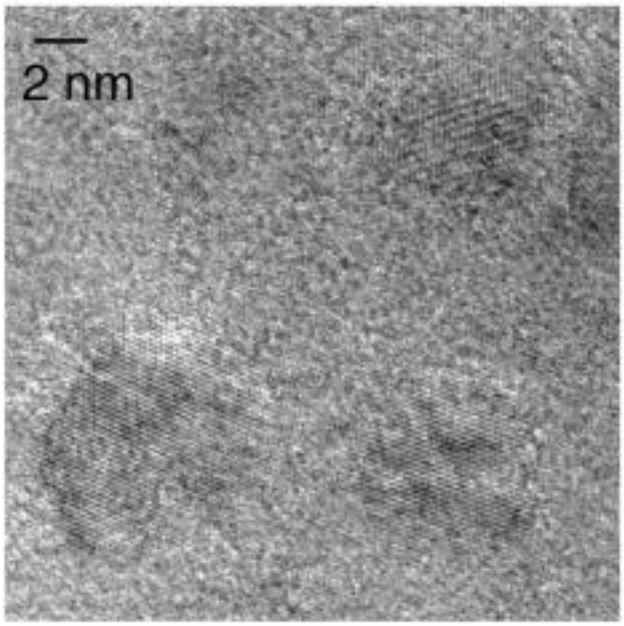

Figure 3 HRTEM image of the $(Co_{0.95}Fe_{0.05})_{88}Zr_7B_4Cu_1$ alloy annealed at 550 °C for 1 hour showing the nanocrystallites and amorphous phase at the grain boundaries

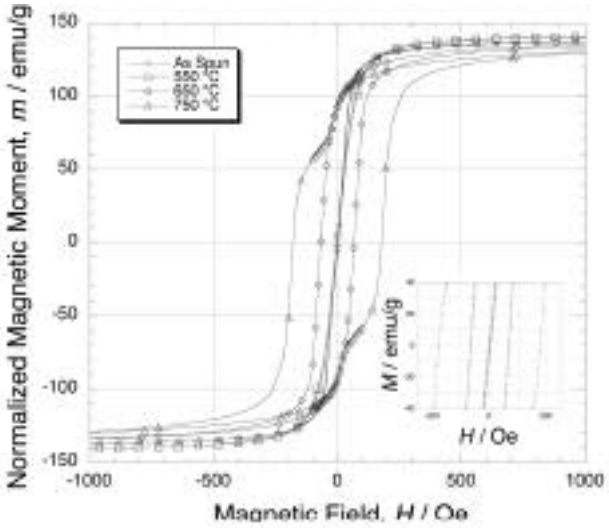

Figure 4 Hysteresis loops for the $(Co_{0.95}Fe_{0.05})_{88}Zr_7B_4$ alloy annealed at 550 °C, 650 °C, and 750 °C for 1 hour.

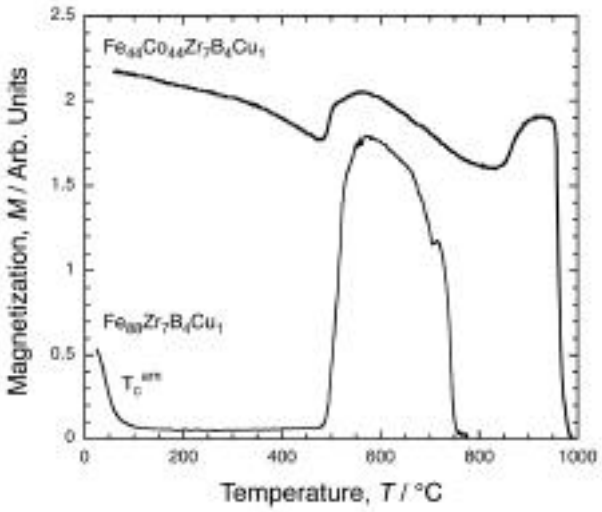

Figure 5 Thermomagnetic data for $(Co_{0.5}Fe_{0.5})_{88}Zr_7B_4Cu_1$ and $Fe_{88}Zr_7B_4Cu_1$ alloys

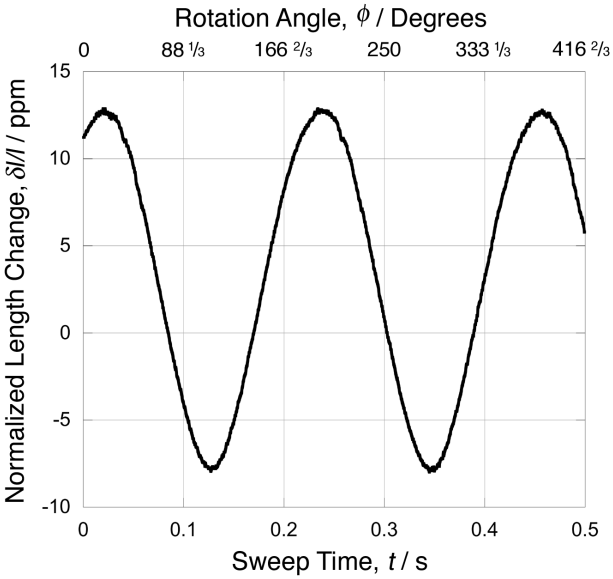

Figure 6 Magnetostriction data for the $(Co_{0.95}Fe_{0.05})_{88}Zr_7B_4$ alloy annealed at 550 °C for 1 hour.